

Sediment focusing in the central equatorial Pacific Ocean

Franco Marcantonio

Department of Geology, Institute for Earth and Ecosystem Sciences, Tulane University, New Orleans, Louisiana

Robert F. Anderson, Sean Higgins, Martin Stute,¹ and Peter Schlosser

Lamont-Doherty Earth Observatory, Department of Earth and Environmental Sciences, Columbia University Palisades, New York

Peter Kubik

Paul Scherrer Institute, Zurich, Switzerland

Abstract. At four sites in the central equatorial Pacific Ocean the flux of extraterrestrial ^3He , determined using the excess ^{230}Th profiling method, is $8 \times 10^{-13} \text{ cm}^3 \text{ STP cm}^{-2} \text{ ka}^{-1}$. This supply rate is constant to within 30%. At these same sites, however, the burial rate of ^3He , determined using chronostratigraphic accumulation rates, varies by more than a factor of 3. The lowest burial rates, which occur north of the equator at 1°N , 139°W are lower than the global average rate of supply of extraterrestrial ^3He by 20% and indicate that sediment winnowing may have occurred. The highest burial rates, which are recorded at the equator and at 2°S , are higher than the rate of supply of extraterrestrial ^3He by 100%, and these provide evidence for sediment focusing. By analyzing several proxies measured in core PC72 sediments spanning the past 450 kyr we demonstrate that periods of maximum burial rates of ^{230}Th , ^3He , ^{10}Be , Ti, and barite, with a maximum peak-to-trough amplitude of a factor of 6, take place systematically during glacial time. However, the ratio of any one proxy to another is constant to within 30% over the entire length of the records. Given that each proxy represents a different source (^{234}U decay in seawater, interplanetary dust, upper atmosphere, continental dust, or upper ocean), our preferred interpretation for the covariation is that the climate-related changes in burial rates are driven by changes in sediment focusing.

1. Introduction

Constant-flux proxies are useful tools in paleoceanography because they enable the reconstruction of past particulate fluxes. Knowledge of these fluxes is crucial if we are to understand the role of the ocean in regulating past climate. For example, one can use changes in the accumulation rates of barite or opal to determine how the productivity of the ocean has varied in the past. Similarly, changes in the accumulation rates of terrigenous dust may yield information about variations in past continental aridity or wind direction. The burial or accumulation rate of any sedimentary constituent is equivalent to its rain rate in addition to any modifications by dissolution and lateral redistribution of sediment (i.e., sediment focusing). Comparing the burial rate of a constant-flux proxy with its known rate of supply enables us to constrain focused deposition of sediments by deep-sea currents [Suman and Bacon, 1989; François *et al.*, 1990, 1993; Frank *et al.*, 1995, 1999; Scholten *et al.*, 1994] as well as changing patterns of sediment focusing in response to reorganization of ocean circulation.

The ^{230}Th profiling method [Bacon, 1984; François *et al.*, 1990; Suman and Bacon, 1989] is based on the assumption that the rain rate of particulate ^{230}Th sinking to the seabed F_{Th} is equivalent to the integrated rate of ^{230}Th production by ^{234}U decay in the overlying water column P_{Th} . This is a reasonable assumption in that ^{230}Th is extremely particle reactive and thus has a short

residence time in the water column (decades). Indeed, F_{Th} is within 30% of P_{Th} over $\sim 70\%$ of the seafloor [Henderson *et al.*, 1999]. Hence the following equation, where F_m is the mass flux of particles, is valid for most deep-marine sediments:

$$xs^{230}\text{Th}(\text{dpm g}^{-1}) = \frac{P_{Th}(\text{dpm cm}^{-2} \text{ kyr}^{-1})}{F_m(\text{g cm}^{-2} \text{ kyr}^{-1})} \quad (1)$$

where dpm is disintegrations per minute. The rain rates of other sedimentary components may also be deduced as follows:

$$F_i = \frac{C_i \beta z}{xs^{230}\text{Th}^0} \quad (2)$$

In (2), F_i is the rain rate of particulate component “ i ”; C_i is the concentration of “ i ” in the sediments; and $\beta z = P_{Th}$, where $\beta = 2.63 \times 10^{-3} \text{ dpm cm}^{-3} \text{ kyr}^{-1}$ and z is the depth of the water column in m. The initial $xs^{230}\text{Th}^0$ concentration of the sediment ($xs^{230}\text{Th}^0$) is decay-corrected using an independent chronology (e.g., $\delta^{18}\text{O}$ stratigraphy).

It is estimated that $\sim 40,000$ tons of interplanetary dust particles (IDPs) fall onto the Earth’s surface every year [Love and Brownlee, 1991]. These IDPs, ranging in size from $1 \mu\text{m}$ to 1 mm , have large surface to volume ratios and thus contain large amounts of noble gases implanted by solar ions [Ozima *et al.*, 1984]. In their study of stratospheric IDPs, Nier and Schlutter [1990] reported average ^3He concentrations of $1.9 \times 10^{-5} \text{ cm}^3 \text{ STP g}^{-1}$ and $^3\text{He}/^4\text{He}$ ratios of 2.4×10^{-4} , several orders of magnitude higher than helium isotope signatures found in the terrestrial environment. Upon entering the Earth’s atmosphere, IDPs $< 30 \mu\text{m}$ in size reach temperatures of only $500^\circ\text{--}800^\circ\text{C}$ [Fraundorf *et al.*, 1982] and hence do not melt. It is this unmelted micrometeoritic fraction that is believed to most likely retain extraterrestrial helium [Ozima *et al.*, 1984].

¹Also at Department of Environmental Sciences, Barnard College, New York, New York.

Over three decades ago, *Merrihue* [1964] discovered extremely high concentrations of ^3He in deep-sea sediment. He suggested that these high concentrations resulted from the fallout of micrometeorites from space. *Farley* [1995] showed that the extraterrestrial ^3He signature is preserved not only in recent sediments but in pelagic sediments as old as 65 Ma. To assess the potential for using ^3He concentrations in sediment as a constant-flux proxy, we used the ^{230}Th profiling method to evaluate the mean flux of ^3He to the seafloor [*Higgins et al.*, 1998; *Marcantonio et al.*, 1995, 1996, 1998, 1999]. Unlike ^{230}Th , which is radioactive with a 75,200 year half-life, ^3He is a stable isotope and therefore useful over longer timescales. Across all of the world's ocean basins at a wide range of latitudes the extraterrestrial ^3He flux, as determined by the ^{230}Th technique, has been calculated to be $\sim 1 \times 10^{-12} \text{ cm}^3 \text{ STP cm}^{-2} \text{ kyr}^{-1}$ with a variability of about $\pm 50\%$ [*Higgins et al.*, 1998].

In our earlier work on sediments from the central equatorial Pacific Ocean [*Marcantonio et al.*, 1996] we hypothesized that in contrast to the constant rain rate of ^{230}Th and ^3He to the ocean floor, the periodic fivefold variations in the burial rates of xs^{230}Th and ^3He over the past 200 kyr were due to lateral advection of sediment. This advection, we hypothesized, may have been caused by a reorganization of deep-sea currents that transported excess particles to a region centered around and just south of the equator. If this sediment focusing hypothesis is valid, there must exist a complementary region from which sediment has been removed. At site C of the Manganese Nodule Project (MANOP site C), north and slightly east of the initial sites we studied, it appears that *Murray* [1987] may have identified such an area. In this contribution, we examine two cores from MANOP site C in order to evaluate whether sediment and ^3He deficits indeed do exist. We then use this analysis to evaluate the focusing hypothesis in more detail.

2. Methodology

Sediment samples from two gravity cores collected in 1984 during the central equatorial Pacific MANOP study were retrieved from the Oregon State University Core and Rock Repository. Cores B18 and B25 are from $1^\circ 3.5' \text{N}$, $138^\circ 48' \text{W}$ (4281 m water depth) and $1^\circ 2.7' \text{N}$, $139^\circ 1' \text{W}$ (4401 m water depth), respectively. Sediment from these cores is composed primarily of carbonate ooze, with minor fractions of opal. Glacial-interglacial stages are characterized by alternating carbonate-rich and carbonate-poor intervals, with enhanced preservation of carbonate during glacial periods.

Helium and thorium isotopes were measured on samples taken from the top 280 cm, an interval that represents ~ 325 kyr in B18 and 266 kyr in B25 (Table 1). In order to remove the biogenic, non-helium-containing fraction of the sediment [*Marcantonio et al.*, 1995], ~ 1.5 g of sediment was leached with ~ 40 mL of 0.3 N acetic acid. Samples were then washed three times with distilled water and dried to a constant weight at 50°C . Helium gas was extracted from the residue, and its ^4He concentration and $^3\text{He}/^4\text{He}$ ratio were measured on an MAP 215-50 mass spectrometer at the Lamont-Doherty Earth Observatory (LDEO). The extraction and mass spectrometric procedures correspond to those followed by *Marcantonio et al.* [1995]. To test the reproducibility of the ^3He concentrations, we developed a central equatorial Pacific sediment "standard." This standard comprises homogenized carbonate sediment taken from a box core retrieved at 0° , 140°W in 1992 during the Joint Global Oceans Flux Study (JGOFS). Sediment at this site is typical of sediment deposited in the central equatorial Pacific. That is, it consists primarily of carbonate ooze, with minor opal, organic carbon, and clay. Seven analyses of this standard yielded ^3He concentrations that are reproducible to within $\pm 8\%$ (1σ) (Table 2). This may be an underestimate of the ^3He

Table 1. The ^3He and $\text{xs}^{230}\text{Th}^0$ Data for Cores B18 and B25

Sample Depth, cm	Age, kyr	$^3\text{He}/^4\text{He}$ ($\times 10^{-5}$)	^3He ($\times 10^{-12}$), $\text{cm}^3 \text{ STP g}^{-1}$	$\text{xs}^{230}\text{Th}^0$ dpm g^{-1}
<i>B18 (1°3'N, 138°48'W)</i>				
1.5	0.3	14.2	1.04	14.1
6.5	4.3	19.3	2.22	17.0
11.5	8.3	11.0	0.45	8.99
21.5	16.3	8.22	0.39	10.4
31.5	24.1	12.1	0.66	10.3
41.5	31.9	15.7	0.65	8.81
51.5	38.9	13.1	0.56	9.52
61.5	45.8	9.62	0.52	9.29
71.5	52.8	9.15	0.43	9.51
81.5	60.8	11.2	1.07	13.8
91.5	71.9	9.95	2.09	25.5
101.5	85.9	10.1	1.77	22.1
111.5	104	10.5	1.43	21.5
121.5	121	7.84	0.66	13.3
131.5	133	8.31	0.64	12.8
141.5	143	7.12	0.61	11.7
151.5	151	9.53	0.69	13.8
161.5	162	8.88	0.80	12.1
171.5	175	9.34	1.27	14.5
181.5	196	8.01	0.91	14.7
191.5	220	8.35	0.44	8.79
201.5	235	8.96	0.64	9.17
211.5	250	7.99	0.89	13.1
221.5	260	7.78	1.66	
231.5	275	8.89	1.32	31.2
241.5	290	10.1	0.84	19.3
251.5	300	7.05	0.42	10.2
261.5	310	5.63	0.40	11.1
271.5	325	7.36	0.47	10.1
271.5	325	7.36	0.47	10.1
<i>B25 (1°2'N, 139°1'W)</i>				
1.5	1.0	27.5		23.3
11.5	7.7	11.2	0.70	14.8
21.5	14.3	8.12	0.48	11.3
31.5	18.0	11.5	0.40	2.49
41.5	25.0	8.29	0.68	15.0
51.5	31.7	10.4	0.63	12.6
61.5	37.5	9.39	0.39	9.69
71.5	43.5	17.4	1.17	10.7
81.5	48.0	15.7	0.77	10.5
91.5	55.5	13.4	1.06	11.6
101.5	64.0	10.6	2.25	25.9
111.5	72.0	7.53	3.28	37.3
121.5	84.0	7.84	2.18	28.1
131.5	100	7.31	1.53	
141.5	116	10.8	1.53	20.1
151.5	128	7.47	0.65	11.3
161.5	137			11.5
171.5	145	7.47	0.76	13.2
181.5	153	6.89	0.73	14.4
191.5	161	7.75	0.71	13.8
201.5	173	11.0	2.56	18.4
211.5	186	5.49	2.37	43.2
221.5	205	7.94	1.14	30.5
231.5	215	10.9	1.68	20.8
241.5	225	9.67	1.13	17.7
251.5	235	10.0	0.69	15.3
261.5	245	7.94	0.61	9.46
271.5	255	8.14	0.88	15.3
281	265	7.24	1.93	25.0
283	266			33.7

^aAge models are from *Murray* [1987]; see discussion in text.

reproducibility, which realistically is closer to a factor of 2 worse (see *Marcantonio et al.* [1999] for a discussion of this point).

Isotope dilution and inductively coupled plasma mass spectrometry (ID-ICP-MS) was used to analyze uranium and thorium at

Table 2. The ^3He Reproducibility Test for Equatorial Pacific “Standard”^a

Equatorial Pacific “Standard”	$^3\text{He}/^4\text{He}$ ($\times 10^{-5}$)	^3He ($\times 10^{-12}$), $\text{cm}^3 \text{STP g}^{-1}$)
1	20.2	0.65
2	19.0	0.67
3	21.9	1.02
4	19.7	0.62
5	19.7	0.75
6	20.6	0.94
7	19.1	0.73
Mean	20.0	0.77
Percent standard error	2	8

^aLocation is 0° , 140°W .

LDEO (VG PlasmaQuad 2). Before dissolution in acid, sediment samples were spiked with ^{229}Th and ^{233}U . The procedure to extract U and Th from the sediment is documented by *Lao et al.* [1992a, 1992b]. Initial excess ^{230}Th activities ($x_s^{230}\text{Th}^0$) were evaluated by correcting for (1) the time since sediment deposition (chronology from *Murray* [1987]), (2) the presence of detrital ^{230}Th (typically 0.1 dpm g^{-1}), and (3) the ingrowth of ^{230}Th by decay of authigenic uranium ($\sim 0.2 \text{ dpm g}^{-1}$). The overall uncertainty of the $x_s^{230}\text{Th}^0$ activity is $<2\%$.

3. Results and Discussion

3.1. Fluxes and Burial Rates

In the central equatorial Pacific (140°W , 0° and 140°W , 2°S) the flux of ^3He estimated by normalizing to $x_s\text{Th}$ is equal to $(7.8 \pm 2.3) \times 10^{-13} \text{ cm}^3 \text{STP cm}^{-2} \text{ kyr}^{-1}$ over the past 200 kyr [*Marcantonio et al.*, 1995, 1996]. Variability of the ^3He flux is not periodic nor is it related to climate change events. However, over the same time period at these equatorial sites, the burial rates for both $x_s^{230}\text{Th}^0$ and ^3He , calculated by multiplying the isotope concentrations by the corresponding bulk sediment accumulation rate derived from $\delta^{18}\text{O}$ records [*Marcantonio et al.*, 1996], exhibit fivefold variations with 100 kyr cyclicity. We interpreted the pronounced variability of these burial rates as being caused by the lateral focusing of sinking particles by deep ocean currents.

Such focusing can be quantified using the ^{230}Th data. *Suman and Bacon* [1989] and *François et al.* [1990] defined a ^{230}Th -derived sediment focusing factor, ψ , as follows:

$$\psi = \frac{\int_0^i [x_s^{230}\text{Th}^0] \rho_b dr}{P_{\text{Th}}(t_1 - t_2)} \quad (3)$$

where r_i is the depth at interval i in the core, t_i is the age at depth i , $[x_s^{230}\text{Th}^0]$ is the concentration of $x_s^{230}\text{Th}^0$ in the sediment, P_{Th} is as defined in (1), and ρ_b is the bulk dry density of the sediment. Sediment focusing factors >1 imply a higher flux of $x_s^{230}\text{Th}$ to the sediments than that expected by production in the water column (i.e., deep-ocean currents laterally advect particles that contain $x_s^{230}\text{Th}$ to the site of interest). Focusing factors <1 indicate that sediment winnowing has taken place (i.e., net export of particles that contain $x_s^{230}\text{Th}$). A down core profile of sediment focusing factors for PC72 is shown in Figure 1. Sediment focusing factors vary from ~ 1 to 4 and show a quasi-100 kyr periodicity.

If the variation in ^{230}Th and ^3He burial rates is due to sediment focusing at the equator and south of the equator, then one would expect that there are complementary regions from which sediments have been winnowed. Two locations at MANOP site C (B18 and B25), north of the sites studied originally, show indications of such winnowing [*Murray*, 1987]. At both sites the concentrations of the

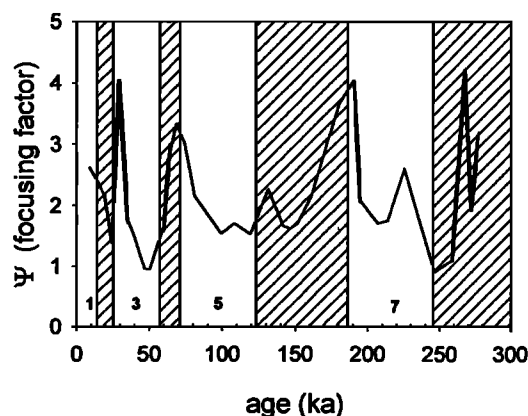


Figure 1. Sediment focusing factors for core PC72 (0° , 140°W) derived using (3). Focusing factors >1 imply a higher flux of $x_s^{230}\text{Th}$ to the sediments than that expected by production in the water column. Hatched regions represent glacial periods (age boundaries from *Imbrie et al.* [1984]).

^3He and $x_s^{230}\text{Th}$ correlate closely (Figure 2), and there is only about a 40% variation in the ratio of the concentration of ^3He to that of $x_s^{230}\text{Th}^0$ (Figure 3). At the MANOP sites the average flux of ^3He using the $x_s^{230}\text{Th}$ profiling method is equal to $(8 \pm 3) \times 10^{-13} \text{ cm}^3 \text{STP cm}^{-2} \text{ kyr}^{-1}$, a rate identical to the average

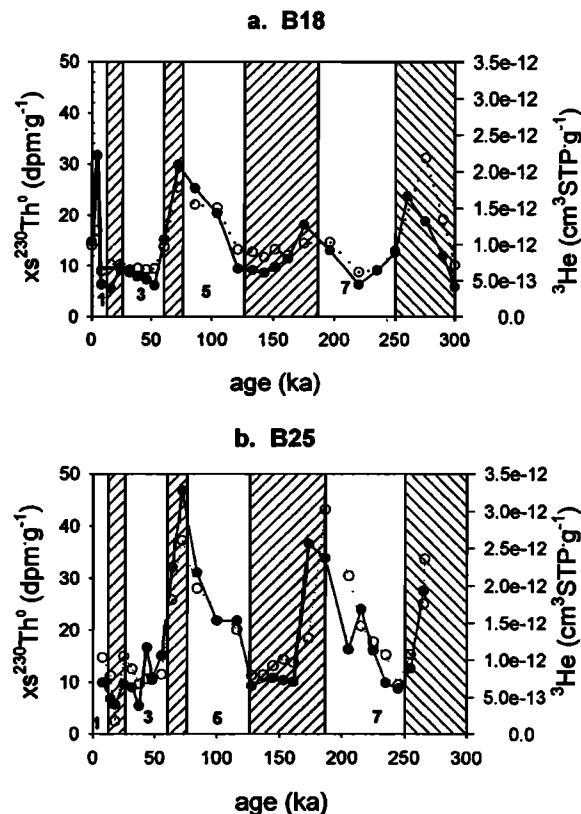


Figure 2. Initial unsupported ^{230}Th (open circles) and ^3He (solid circles) concentrations plotted against age for sediments from cores (a) B18 ($1^\circ 3.5'\text{N}$, $138^\circ 48'\text{W}$, 4281 m water depth) and (b) B25 ($1^\circ 2.7'\text{N}$, $139^\circ 1'\text{W}$, 4401 m water depth). Hatched regions represent glacial periods (age boundaries from *Imbrie et al.* [1984]).

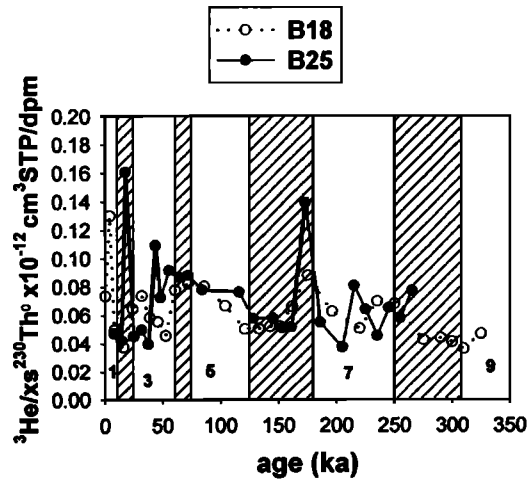


Figure 3. The $^3\text{He}/x\text{s}^{230}\text{Th}^0$ ratios for sediment from cores B18 (open circles) and B25 (solid circles) plotted against age. Hatched regions represent glacial periods (age boundaries from *Imbrie et al.* [1984]).

measured farther south at the equator and 2°S [*Marcantonio et al.*, 1996].

Using age model-derived sediment accumulation rates, we can calculate the burial rates of ^3He and ^{230}Th and assess whether there is evidence for sediment redistribution at MANOP site C. *Murray* [1987] constructed age models for the first 200 kyr of cores B18 and B25 (shown in Table 1) by correlating CaCO_3 concentrations with nearby core W8402A-14GC, which he dated using $\delta^{18}\text{O}$ stratigraphy. Prior to 200 ka, to lengthen the age model, we used correlations between CaCO_3 concentrations with core PC72, also dated using $\delta^{18}\text{O}$ stratigraphy. Average sediment mass accumulation rates (MARs) are 0.59 and 0.64 $\text{g cm}^{-2} \text{kyr}^{-1}$ for cores B18 and B25, respectively. These estimates are robust in that they do not depend on a detailed point-by-point age model. The average MARs lead to average ^3He burial rates of 5.2 and $7.8 \times 10^{-13} \text{cm}^3 \text{STP cm}^{-2} \text{kyr}^{-1}$ (Table 3) and average ^{230}Th burial rates of 8.1 and 11.6 $\text{dpm cm}^{-2} \text{kyr}^{-1}$ for cores B18 and B25, respectively. In core B18 the average ^{230}Th and ^3He burial rates are both 20% lower than those expected from local production for xsTh (constrained by P_{Th}) as well as from the supply from outer space for ^3He (constrained by the average global $^3\text{He}/x\text{s}^{230}\text{Th}$ ratio). The burial rates of ^{230}Th and ^3He in B25 sediments, calculated in the same way, are identical to those expected (Table 3) for equilibrium conditions (i.e., no sediment focusing or winnowing). Sediments north of the equator yield results that are in stark contrast to those obtained for sediments at 0° and 2°S (PC72 and PC18 [*Marcantonio et al.*, 1996]). In these cores the average ^{230}Th burial rate is twice that expected by local production, and the average ^3He burial rate is twice that expected by the supply from space (Table 3).

Table 3. Average ^3He Accumulation Rates^a

Core	^{230}Th Normalized (^3He Rain Rate)	$\delta^{18}\text{O}$ Normalized (^3He Burial Rate)
B18 (1°3'N, 138°48'W)	6.9 ± 2.2	5.2
B25 (1°2'N, 139°1'W)	8.2 ± 3.5	7.8
TT013-PC72 (0°, 140°W)	7.3 ± 3.1	14.8
TT013-PC18 (2°S, 140°W)	8.6 ± 2.7	14

^aAccumulation rates are $\times 10^{-13} \text{cm}^3 \text{STP cm}^{-2} \text{kyr}^{-1}$.

Hence, while the xsTh-normalized ^3He fluxes values are constant for all equatorial sites (within uncertainty), the stratigraphically defined (^{18}O) ^3He burial rates values vary from site to site by nearly a factor of 3 (Table 3). Whereas the constant xsTh-normalized ^3He fluxes imply a constant supply rate of extraterrestrial ^3He from space, we believe the variation in ^3He burial rates at the different sites is likely due to lateral transport of sediment along the seafloor. North of the equator (1°N) the average ^3He burial rate, which is lower than expected from the extraterrestrial ^3He flux, indicates that some winnowing may have taken place. Farther south, at 0° and 2°S, the average ^3He burial rate is greater than the rate of supply of extraterrestrial ^3He by about a factor of 2, a value that reflects net sediment focusing. Identical arguments can be

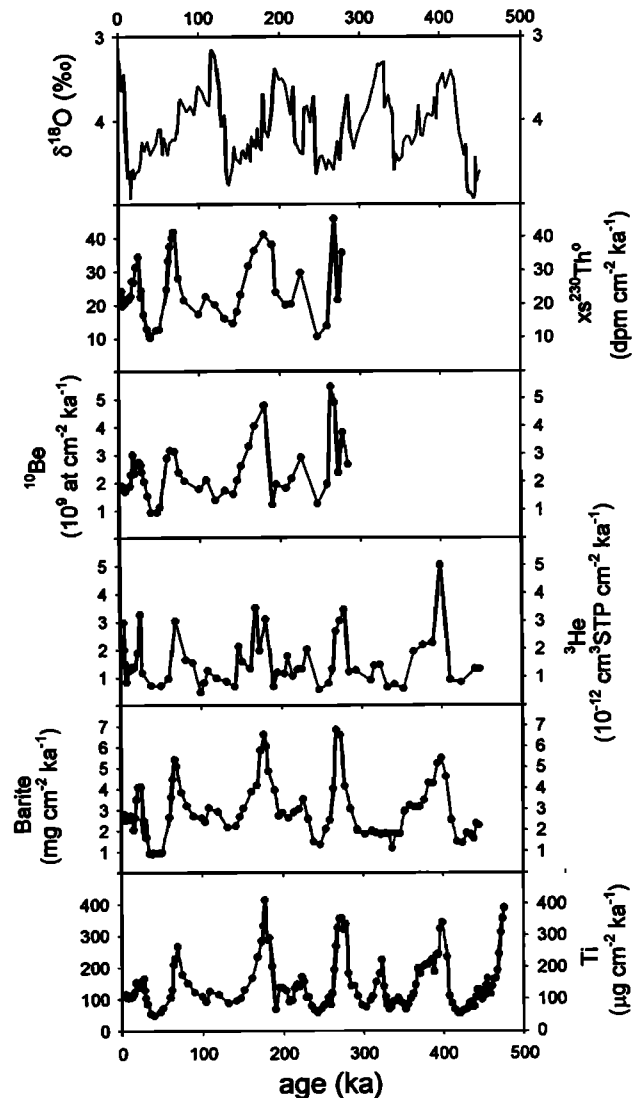


Figure 4. Multiproxy record for core PC72 (0°, 140°W). The $\delta^{18}\text{O}$ [*Marcantonio et al.*, 1996], $x\text{s}^{230}\text{Th}^0$ burial rate [*Marcantonio et al.*, 1996], ^{10}Be burial rate (this study), ^3He burial rate [*Marcantonio et al.*, 1996], barite burial rate [*Paytan et al.*, 1996], and Ti burial rate [*Murray et al.*, 1995] plotted against age. The production rate of xs ^{230}Th at this site is equal to 11.3 $\text{dpm cm}^{-2} \text{kyr}^{-1}$. The complete data set (^{10}Be and ^{230}Th) for sediments and sediment trap samples will eventually be served on the U.S. JGOFS data web site (<http://usjgofs.whoi.edu>). Until then, these data can be obtained by request to R. F. Anderson.

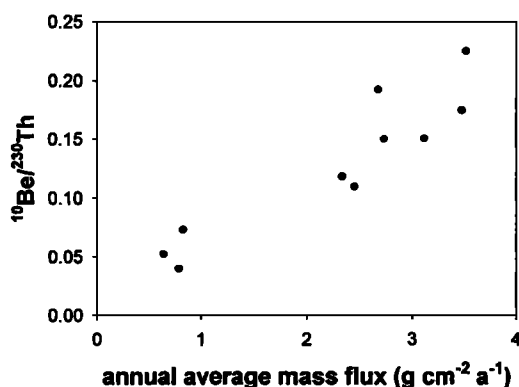


Figure 5. Particulate $^{10}\text{Be}/^{230}\text{Th}$ ratio versus annual average particulate mass flux. Particles were collected in sediment traps deployed near our core sites, along a transect normal to the equator at 140°W , from 9°N to 12°S [Honjo *et al.*, 1995].

made with respect to the average ^{230}Th burial rates and the potential winnowing and focusing of sediment.

The extended record for PC72 (0°) exhibits a regular 100 kyr cyclic pattern of increased burial of ^3He and $x\text{s}^{230}\text{Th}$ over the past 450 kyr [Marcantonio *et al.*, 1996]. In addition to Th and He, other proxies have also been measured in this core (^{10}Be (this study), Ti [Murray *et al.*, 1995], and barite [Paytan *et al.*, 1996]). Multi-proxy results are plotted in Figure 4. Periods of maximum accumulation rates of ^{230}Th , ^3He , ^{10}Be , Ti, and barite take place during glacial periods. More specifically, extrema in the accumulation rates of all of the proxies occur regularly during the middle part of the growth of continental ice sheets (Figure 4; increasing $\delta^{18}\text{O}$). Furthermore, the ratio of any one proxy to another is constant to within $\pm 30\%$ over 450 kyr. This is a startling discovery because the sources of each proxy are completely independent of one another. The ^{230}Th derives from the deep-ocean water column, ^3He derives from IDPs that originate in space, ^{10}Be derives from the upper atmosphere, Ti derives from windblown dust from the continents, and barite derives from sinking biogenic debris. The correlations argue strongly for an oceanic process, such as sediment focusing, which acts upon each proxy in the same way.

3.2. Alternative Processes for Variable ^3He and ^{230}Th Inventories in the Sediment

There are two possible alternatives to the sediment focusing hypothesis: (1) systematic errors in the ^{18}O age model that are introduced by carbonate dissolution or (2) genuine variability in the accumulation rate of all tracers caused by changes in productivity. The first possibility would have serious ramifications for studies of past accumulation rates in the equatorial Pacific as well as for other sites where periodic calcium carbonate dissolution occurs. Since most paleoaccumulation rate studies of biogenic and eolian material rely on $\delta^{18}\text{O}$ age models, it would be difficult to evaluate past changes in ocean productivity or wind strength and aridity in response to climate change. However, the $\delta^{18}\text{O}$ record from PC72 (Figure 4) matches the global average record (SPEC-MAP [Martinson *et al.*, 1987]) very well. Indeed, the lack of hiatuses in the PC72 $\delta^{18}\text{O}$ record is evidence for a reliable $\delta^{18}\text{O}$ -based age model in that artifacts in the model due to dissolution are probably minimal.

A productivity hypothesis is preferred by Paytan *et al.* [1996] to explain the variations in barite accumulation rate. In this hypothesis, changes in productivity and export flux of sinking particles, as inferred from the barite record, regulate the burial rate of all the other tracers by changing their rate of removal from the water column by scavenging [Thomas *et al.*, 2000]. We believe this to be

an unreasonable explanation for two principle reasons. First, the maximum apparent $x\text{s}^{230}\text{Th}$ flux/production ratios in PC72 (~ 4 ; Figures 1 and 4) exceed the highest ratios observed in sediment traps anywhere in the modern ocean by more than a factor of 2 [Yu, 1994]. Attributing $x\text{s}^{230}\text{Th}$ fluxes this large to scavenging is unreasonable because the flux of $x\text{s}^{230}\text{Th}$ scavenged from the water column is relatively insensitive to changes in particle flux [François *et al.*, 1990; Yu, 1994]. Second, the tight coupling of the apparent accumulation rates of all proxies requires that their scavenging from the water column responds to variable particle flux with exactly the same sensitivity. This seems unreasonable, given the diverse sources and chemical properties of the various tracers.

To illustrate the point above, we compare the scavenging behavior of ^{10}Be to that of ^{230}Th . As already described, Th is sufficiently particle reactive that throughout the ocean, ^{230}Th is scavenged and removed to sediments at a rate nearly equal to its production by U decay in the water column. In contrast to Th, scavenging of more soluble tracers, such as ^{10}Be , increases with increasing particle flux, leading to the well-established pattern of boundary scavenging, where scavenging of ^{10}Be is enhanced in

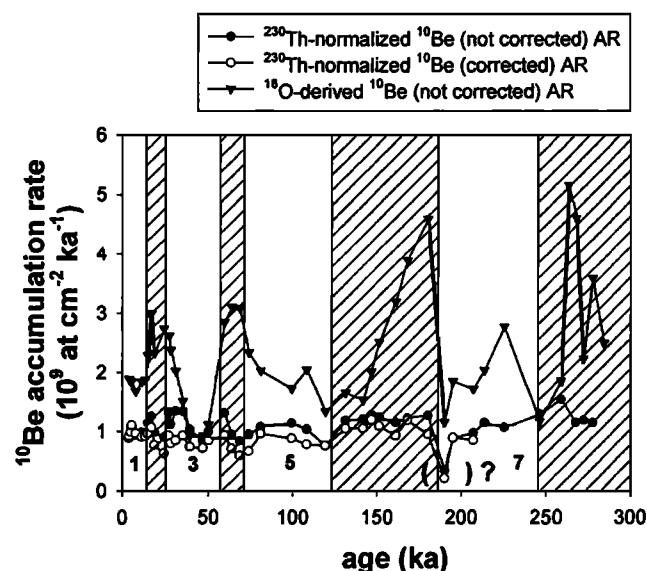


Figure 6. Down core ^{10}Be accumulation rates for PC72 (0° , 140°W). The ^{18}O -derived ^{10}Be accumulation rate is equal to the ^{10}Be concentration multiplied by the ^{18}O -derived sediment mass accumulation rate. The ^{230}Th -normalized ^{10}Be accumulation rate is calculated using (2) and is numerically equivalent to the $^{10}\text{Be}/x\text{s}^{230}\text{Th}$ ratio multiplied by the ^{230}Th production rate. Because the ^{230}Th production rate is constant, the ^{230}Th -normalized ^{10}Be accumulation rate should have the same sensitivity to particle flux as the $^{10}\text{Be}/^{230}\text{Th}$ ratio does (e.g., Figure 5). The ^{230}Th -normalized ^{10}Be fluxes are shown with and without correction for past changes in production rate of cosmogenic nuclides due to changes in Earth's magnetic field strength. An algorithm to describe the global average production rate of ^{10}Be over the past 205 kyr presented by Frank *et al.* [1997] was used to normalize our ^{230}Th -normalized ^{10}Be fluxes to the modern ^{10}Be production rate. Because Frank's algorithm is defined only to 205 kyr, only the uncorrected ^{10}Be fluxes are shown prior to that time. Hatched regions represent glacial periods (age boundaries from Imbrie *et al.* [1984]). Although the data point enclosed in parentheses is anomalously low, we cannot find any reason to discard it and have designated the point with a question mark.

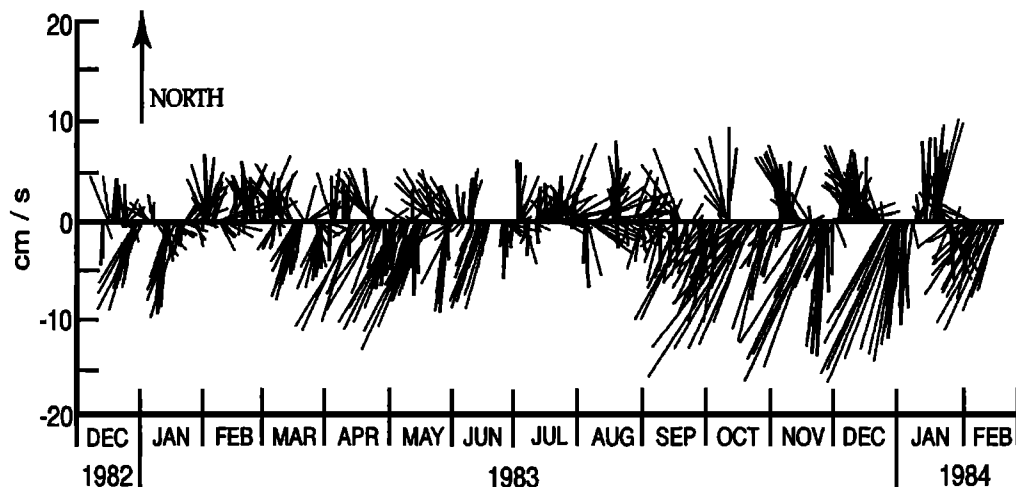


Figure 7. Bottom current meter record from Manganese Nodule Project (MANOP) site C for December 1982 to February 1984. Current meter results were provided by J. Dymond and R. Collier (Oregon State University).

ocean margin regions of high particle flux [e.g., *Anderson et al.*, 1990; *Lao et al.*, 1992a]. Because of the contrasting sensitivity to particle flux by the scavenging of Th and of Be, one finds in the modern ocean that the particulate $^{10}\text{Be}/^{230}\text{Th}$ ratio tends to increase with increasing particle flux. This point is illustrated by results from sediment traps deployed near our core sites, along a transect normal to the equator at 140°W , from 9°N to 12°S [*Honjo et al.*, 1995], where we find that the particulate $^{10}\text{Be}/^{230}\text{Th}$ ratio bears a strong relationship to annual particle flux (Figure 5).

If the variable deposition of the tracers studied in PC72 (Figure 4) were regulated by the intensity of scavenging which, in turn, derives directly from the flux of biogenic particles, then we would expect the $^{10}\text{Be}/^{230}\text{Th}$ ratio to increase at times of greater particle flux. To the extent that the sediment trap results (Figure 5) provide a valid calibration of the sensitivity of the particulate $^{10}\text{Be}/^{230}\text{Th}$ ratio to changes in particle flux back through time, we expect a near 1:1 relationship between the decay-corrected $^{10}\text{Be}/^{230}\text{Th}$ ratio in PC72 and the contemporary particle flux. In fact, the down core record of $^{10}\text{Be}/^{230}\text{Th}$ in PC72 is nearly featureless (Figure 6) and clearly lacks any detectable maxima at times of peak ^{18}O -derived accumulation rates during glacial periods. Hence the maxima in ^{18}O -derived ^{10}Be burial rates are not caused by enhanced scavenging due to a large change in the flux of biogenic particles. Extrapolating to the other tracers, we further conclude that the coherent maxima in the burial rates of all the proxies (Figure 4) are not the product of enhanced glacial productivity and scavenging from the water column.

3.3. Corroborating Evidence for Sediment Focusing

There is corroborating evidence in the literature that supports the sediment focusing interpretation. For example, comparing the pattern of particulate organic carbon fluxes across the equator with the pattern of phytodetritus accumulating on the seabed suggests that focusing of the phytodetritus has occurred. Sediment trap particulate flux data from the central equatorial Pacific (140°W) indicate a nearly uniform average annual particle rain rate between 5°S and 5°N [*Honjo et al.*, 1995, Figure 3]. However, in this same transect (140°W) over the same range of latitudes, ocean bottom phytodetritus abundances peak at the equator [*Smith et al.*, 1996, Figure 2]. Indeed, the largest concentration of flocculent phytodetritus occurs between 2°N and 2°S . The concentration of this fine-grained material on the

sea bottom decreases steeply as distance from the equator increases. The contrast between particle rain rates and phytodetritus abundances is consistent with the idea that phytodetritus is being focused toward the equator. Further evidence that this may be the case comes from pore water profiles from the same region [*Hammond et al.*, 1996]. Diffusive fluxes of oxygen reveal that the benthic oxidation of organic carbon at 4° and 5°N is only about one third of the rate of benthic carbon oxidation within 2° of the equator [*Hammond et al.*, 1996] despite the nearly uniform particulate organic carbon (POC) rain across the region collected by sediment traps. This suggests that some POC has been lost from the northern sites by sediment winnowing.

Current meters deployed at MANOP site C from December 1982 to February 1984 show bottom currents at a depth of 4400 m (50 m above the bottom) in excess of 10 cm s^{-1} moving from NE to SW during much of the year (Figure 7; current meter data provided by J. Dymond and R. Collier (personal communication, 1998)). *Lampitt* [1985] has shown that in order for phytodetritus to be moved on the seafloor, water currents must be in excess of 7 cm s^{-1} . Maximum current speeds at MANOP site C are in excess of 20 cm s^{-1} and directed toward the SW. While these results are insufficient to conclude that particles deposited near MANOP site C serve as a source of sediment focused to the locations of PC72 (equator) and PC18 (2°S), the amplitude and direction of the bottom currents at MANOP site C show the feasibility of the requisite sediment transport. Further studies are needed to characterize completely the timescale and space scale of sediment transport in this region.

Further evidence for winnowing and erosion just north of the equator in the central equatorial Pacific comes from a JGOFS piston core recovered at 5°N , 140°W (TT013-PC105). This core contains Tertiary chalk below a depth of $\sim 2\text{ m}$ (M. Leinen, personal communication, 1998). Above 2 m, there is either a hiatus or multiple erosional surfaces, indicating removal of sediment by bottom currents. Corroborating geophysical evidence, in the form of deep-tow surveys, suggests that bottom currents have winnowed sediments at 4°N , 136°W , close to the equatorial sites studied here [*Mayer*, 1981].

3.4. Implications for Paleooceanographic Interpretations

Failure to account for sediment focusing processes can have a severe impact on paleooceanographic interpretations. For example, *Paytan et al.* [1996] interpret ^{18}O -derived barite burial rates at

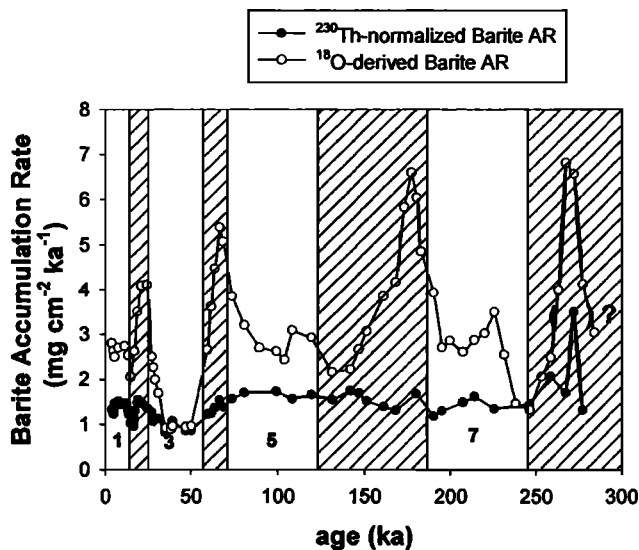


Figure 8. Down core barite accumulation rates for PC72 (0° , 140° W). The ^{18}O -derived barite accumulation rate is equal to the barite concentration multiplied by the ^{18}O -derived sediment mass accumulation rate. The barite concentration data are from Paytan [1995]. Paytan's [1995] original barite data, determined at 10 cm depth intervals, were interpolated onto the depths of our ^{230}Th samples in order to calculate ^{230}Th -normalized barite accumulation rates. Hatched regions represent glacial periods (age boundaries from Imbrie et al. [1984]). Although the data point enclosed in parentheses is anomalously low, we cannot find any reason to discard it and have designated the point with a question mark.

face value and infer that there have been distinct climate-related changes in barite accumulation (i.e., productivity), with a maximum peak-to-trough amplitude of a factor of 6 and maxima occurring systematically during glacials (Figure 4). Normalizing to ^{230}Th eliminates most of the variability in barite accumulation rate (Figure 8), although there remains some small systematic variability (e.g., the minimum between 30 and 55 kyr). More important, however, is that the glacial maxima in export production inferred from ^{18}O -derived barite burial rates are absent. This is consistent with the Th-normalized ^{10}Be accumulation rate, which likewise shows no evidence for increased production (i.e., particle flux, Figure 6) during glacial times. Given the consistent records from two independent proxies (^{10}Be and barite), we conclude that export production in the central equatorial Pacific Ocean was not significantly greater than today during glacial periods. Evidence in support of higher glacial productivity, inferred from this region in previous studies, is biased by the failure to recognize the systematic climate-related pattern of variable sediment focusing. A more complete analysis of the paleoproductivity record from this region using a compre-

hensive multiproxy approach and additional cores will be developed in a future publication.

The sediment focusing hypothesis has further implications for paleoceanography given that periods of maximum sediment focusing correspond to periods of minimum calcium carbonate concentration [Marcantonio et al., 1996] in the sediments. Berelson et al. [1997] have shown that CaCO_3 dissolution in equatorial Pacific sediments is influenced more by bottom water undersaturation than by metabolically produced CO_2 . Hence, changing bottom water chemistry, as recorded by CaCO_3 dissolution, may be linked to changes in deep-sea circulation, as recorded by the sediment focusing. This, in turn, could lead to variations in the distribution of CO_2 between the ocean and the atmosphere.

4. Conclusions

Multiple lines of evidence presented here provide a strong case for sediment focusing in the equatorial Pacific Ocean over the last several hundred thousand years. More work is needed before we understand the nature of the deep-sea currents responsible for the alternating pattern of sediment focusing and sedimentary carbonate dissolution cycles. However, the linkage between sediment focusing and bottom water chemistry (carbonate ion concentration, as manifest by CaCO_3 dissolution), over glacial-interglacial times, points toward a potential connection between deep-ocean circulation and the ocean-atmosphere carbon cycle [e.g., Broecker and Peng, 1989; Keir, 1995].

Similar responses among a suite of particulate tracers of differing origin (^{230}Th , ^3He , Ti, ^{10}Be , and barite) suggest that focusing in this region does not fractionate among different types of particles, for example, through hydrodynamic sorting. The pronounced maximum in phytodetritus abundance observed near the equator may indicate that the focusing mechanism acts primarily on phytodetritus before these large flocculant aggregates become incorporated into the bulk sediment. Focusing of aggregated material containing all types of particles could produce the observed pattern of accumulation common to all of the tracers.

In many paleoceanographic studies, interpretations rely on sediment accumulation rates derived from $\delta^{18}\text{O}$ stratigraphy. Such accumulation rates, unlike those derived using constant-flux proxies, are sensitive to the effects of sediment focusing. As shown here, the effects of sediment focusing may not be evident in $\delta^{18}\text{O}$ records. Investigators must be wary of the potential influence of these effects on their results.

Acknowledgments. Support for this work was derived from NSF grants OCE90-22301, OCE97-14898, and OCE97-11870. LDEO noble gas laboratory support was provided by the W. M. Keck Foundation and NSF EAR 90-18987. Samples were generously provided by the curators at the Oregon State University and University of Rhode Island core repositories. We thank J. Dymond and R. Collier for sharing their current meter results (Figure 7) with us, Dave Murray for useful discussions, and Martin Frank and an anonymous referee for constructive reviews. We are grateful to Y. Lao for help with the analyses.

References

- Anderson, R. F., Y. Lao, W. S. Broecker, S. E. Trumbore, H. J. Hofmann, and W. Wolfli, Boundary scavenging in the Pacific Ocean: A comparison of ^{10}Be and ^{231}Pa , *Earth Planet. Sci. Lett.*, **90**, 287–304, 1990.
- Bacon, M. P., Glacial to interglacial changes in carbonate and clay sedimentation in the Atlantic Ocean estimated from ^{230}Th measurements, *Isot. Geosci.*, **2**, 97–111, 1984.
- Berelson, W. M., et al., Biogenic budgets of particle rain, benthic remineralization and sediment accumulation in the equatorial Pacific, *Deep Sea Res., Part II*, **44**, 2251–2281, 1997.
- Broecker, W. S., and T.-H. Peng, The cause of the glacial to interglacial atmospheric CO_2 change: A polar alkalinity hypothesis, *Global Biogeochem. Cycles*, **3**, 215–239, 1989.
- Farley, K. A., Cenozoic variations in the flux of interplanetary dust recorded by ^3He in a deep-sea sediment, *Nature*, **376**, 153–156, 1995.
- François, R., M. P. Bacon, and D. O. Suman, ^{230}Th profiling in deep-sea sediments: High-resolution records of flux and dissolution of carbonate in the equatorial Atlantic during the last 24,000 years, *Paleoceanography*, **5**, 761–787, 1990.
- François, R., M. P. Bacon, M. A. Altabet, and L. D. Labeyrie, Glacial/interglacial changes in sediment rain rate in the SW Indian sector of subantarctic waters as recorded by ^{230}Th ,

- ²³¹Pa, U, and δ^{15} N, *Paleoceanography*, 8, 611–629, 1993.
- Frank, M., A. Eisenhauer, W. J. Bonn, P. Walter, H. Grobe, P. W. Kubik, B. Dittrich-Hannen, and A. Mangini, Sediment redistribution versus paleoproductivity change: Weddell Sea Margin sediment stratigraphy for the last 250,000 years deduced from ²³⁰Th_{ex}, ¹⁰Be and biogenic barium profiles, *Earth Planet. Sci. Lett.*, 136, 559–573, 1995.
- Frank, M., B. Schwarz, S. Baumann, P. W. Kubik, M. Suter, and A. Mangini, A 200 kyr record of cosmogenic radionuclide production rate and geomagnetic field intensity from ¹⁰Be in globally-stacked deep-sea sediments, *Earth Planet. Sci. Lett.*, 149, 121–129, 1997.
- Frank, M., R. Gersonde, and A. Mangini, Sediment redistribution, ²³⁰Th-normalization and implications for the reconstruction of particle flux and export paleoproductivity, in *Use of Proxies in Paleoceanography. Examples From the South Atlantic*, edited by G. Fischer and G. Wefer, pp. 409–426, Springer-Verlag, New York, 1999.
- Fraundorf, P., T. Lyons, and P. Schubert, The survival of solar flare tracks in interplanetary dust silicates on deceleration in the Earth's atmosphere, *J. Geophys. Res.*, 87, 409–412, 1982.
- Hammond, D. E., J. McManus, W. M. Berelson, T. E. Kilgore, and R. H. Pope, Early diagenesis of organic material in equatorial Pacific sediments: Stoichiometry and kinetics, *Deep Sea Res., Part II*, 43, 1365–1412, 1996.
- Henderson, G. M., C. Heinze, R. F. Anderson, and A. M. E. Winguth, Global distribution of the ²³⁰Th flux to ocean sediments constrained by GCM modelling, *Deep Sea Res., Part I*, 46, 1861–1893, 1999.
- Higgins, S., F. Marcantonio, R. F. Anderson, M. Stute, and P. Schlosser, A global estimate of the late Quaternary (300 kyr) IDP flux based on ³He/²³⁰Th ratios in marine sediments, *Eos Trans. AGU*, 79(45), Fall Meet. Suppl., F50, 1998.
- Honjo, S. J., J. Dymond, R. Collier, and S. J. Manganini, Export production of particles to the interior of the equatorial Pacific Ocean during the 1992 EqPac experiment, *Deep Sea Res., Part II*, 42, 831–870, 1995.
- Imbrie, J., J. D. Hays, D. G. Martinson, A. McIntyre, A. C. Mix, J. J. Morley, N. G. Pisias, W. L. Prell, and N. J. Shackleton, The orbital theory of Pleistocene climate: Support from a revised chronology of the δ^{18} O record, in *Milankovitch and Climate*, edited by A. L. Berger, pp. 269–305, D. Reidel, Norwell, Mass., 1984.
- Keir, R. S., Is there a component of Pleistocene CO₂ change associated with carbonate dissolution cycles?, *Paleoceanography*, 10, 871–880, 1995.
- Lampitt, R. S., Evidence for the seasonal deposition of detritus to the deep-sea floor and its subsequent resuspension, *Deep Sea Res.*, 32, 885–897, 1985.
- Lao, Y., R. F. Anderson, and W. S. Broecker, Boundary scavenging and deep-sea sediment dating: Constraints from excess ²³⁰Th and ²³¹Pa, *Paleoceanography*, 7, 783–798, 1992a.
- Lao, Y., R. F. Anderson, W. S. Broecker, S. E. Trumbore, H. J. Hofmann, and W. Wolfli, Transport and burial rates of ¹⁰Be and ²³¹Pa in the Pacific Ocean during the Holocene period, *Earth Planet. Sci. Lett.*, 113, 173–189, 1992b.
- Love, S. G., and D. E. Brownlee, A direct measurement of the terrestrial mass accretion rate of cosmic dust, *Science*, 262, 550–553, 1991.
- Marcantonio, F., N. Kumar, M. Stute, R. F. Anderson, M. A. Seidl, P. Schlosser, and A. Mix, A comparative study of accumulation rates derived by He and Th isotope analysis of marine sediments, *Earth Planet. Sci. Lett.*, 133, 549–555, 1995.
- Marcantonio, F., R. F. Anderson, M. Stute, N. Kumar, P. Schlosser, and A. Mix, Extraterrestrial ³He as a tracer of marine sediment transport and accumulation, *Nature*, 383, 705–707, 1996.
- Marcantonio, F., S. Higgins, R. F. Anderson, M. Stute, P. Schlosser, and E. T. Rasbury, Terrigenous helium in deep-sea sediments, *Geochim. Cosmochim. Acta*, 62, 1535–1543, 1998.
- Marcantonio, F., K. K. Turekian, S. Higgins, R. F. Anderson, M. Stute, and P. Schlosser, The accretion rate of extraterrestrial ³He based on oceanic ²³⁰Th flux and the relation to Os isotope variation over the past 200,000 years in an Indian Ocean core, *Earth Planet. Sci. Lett.*, 170, 157–168, 1999.
- Martinson, D. G., N. G. Pisias, J. D. Hays, J. Imbrie, T. C. Moore, and N. J. Shackleton, Age dating and the orbital theory of the ice ages: Development of a high-resolution 0–300,000 year chronostratigraphy, *Quat. Res.*, 27, 1–29, 1987.
- Mayer, L., Erosional troughs in deep-sea carbonates and their relationship to basement structure, *Mar. Geol.*, 39, 59–80, 1981.
- Merrhue, C., Rare gas evidence for cosmic dust in modern Pacific red clay, *Ann. N. Y. Acad. Sci.*, 119, 351–367, 1964.
- Murray, D., Spatial and temporal variations in sediment accumulation in the central tropical Pacific Ocean, Ph.D. thesis, Oregon State Univ., Corvallis, 1987.
- Murray, R. W., M. Leinen, D. W. Murray, A. C. Mix, and C. W. Knowlton, Terrigenous Fe input and biogenic sedimentation in the glacial and interglacial equatorial Pacific Ocean, *Global Biogeochem. Cycles*, 9, 667–684, 1995.
- Nier, A. O., and D. J. Schlutter, Helium and neon isotopes in stratospheric particles, *Me-teoritics*, 25, 263–267, 1990.
- Ozima, M., M. Takayanagi, S. Zashu, and S. Amari, High ³He/⁴He ratio in ocean sediments, *Nature*, 311, 448–450, 1984.
- Paytan, A. M., Marine barite, a recorder of ocean chemistry, productivity, and circulation, Ph.D. thesis, Univ. of Calif., San Diego, 1995.
- Paytan, A. M., M. Kastner, and F. P. Chavez, Glacial to interglacial fluctuations in productivity in the equatorial Pacific as indicated by marine barite, *Science*, 274, 1355–1357, 1996.
- Scholten, J. C., R. Botz, H. Paetsch, and P. Stoffers, ²³⁰Th_{ex} flux into Norwegian-Greenland Sea sediments: Evidence for lateral sediment transport during the past 300,000 years, *Earth Planet. Sci. Lett.*, 121, 111–124, 1994.
- Smith, C. R., D. J. Hoover, S. E. Doan, R. H. Pope, D. J. DeMaster, F. C. Dobbs, and M. A. Altabet, Phytodetritus at the abyssal seafloor across 10 degrees of latitude in the central equatorial Pacific, *Deep Sea Res. Part II*, 43, 1309–1338, 1996.
- Suman, D. O., and M. P. Bacon, Variations in Holocene sedimentation in the North American Basin determined by ²³⁰Th measurements, *Deep Sea Res.*, 36, 869–878, 1989.
- Thomas, E., K. K. Turekian, and K.-Y. Wei, Productivity control of fine particle transport to equatorial Pacific sediment, *Global Biogeochem. Cycles*, 14, 945–955, 2000.
- Yu, E.-F., Variations in the particulate flux of ²³⁰Th and ²³¹Pa and paleoceanographic applications of the ²³¹Pa/²³⁰Th ratio, Ph.D. thesis, Woods Hole Oceanogr. Inst./Mass. Inst. of Technol., Woods Hole, Mass., 1994.

R. F. Anderson, S. Higgins, P. Schlosser, and M. Stute, Lamont-Doherty Earth Observatory and Department of Earth and Environmental Sciences, Columbia University, Palisades, NY 10964.

P. Kubik, Paul Scherrer Institute, c/o Institute of Particle Physics, Zurich, HPK H30, ETH Hoenggerberg, CH-8093 Switzerland.

F. Marcantonio, Department of Geology, Institute for Earth and Ecosystem Sciences, Tulane University, New Orleans, LA 70118. (fmarcan@tulane.edu)

(Received May 8, 2000;
revised January 16, 2001;
accepted March 7, 2001.)